Received March 2000
Revised July 2000
Accepted August 2000

Mixed convection in a square cavity due to heat generating rectangular body

Effect of cavity exit port locations

S.Z. Shuja, B.S. Yilbas and M.O. Iqbal
King Fahd University of Petroleum and Minerals, Dhahran, Saudi Arabia

Keywords *Convection, Square cavity, Exit port, Heat transfer*

Abstract *Flow in the cavity with heat generating body finds wide domestic and industrial applications. The heat transfer characteristics and the irreversibility generated in the cavity depend on mainly the cavity size, aspect ratio of the heat generating body, and inlet/exit port locations. In the present study, effect of exit port locations on the heat transfer characteristics and irreversibility generation in a square cavity with heat generating body is investigated. A numerical simulation is carried out to predict the velocity and temperature fields in the cavity. To examine the effect of solid body aspect ratio on the heat transfer characteristics two extreme aspect ratios (0.25 and 4.0) are considered in the analysis. Fifteen different locations of exit port are introduced while air is used as an environment in the cavity. It is found that non-uniform cooling of the solid body occurs for exit port location numbers of 13 and beyond. In this case, heat transfer reduces while irreversibility increases in the cavity. These findings are valid for both aspect ratios of the solid body.*

Nomenclature

A = cross-sectional area of solid body (m^2)
a = aspect ratio
b = length of protruding body (m)
c = height of protruding body (m)
h = heat transfer coefficient (W/m^2K)
I = irreversibility (W/m^3)
k = thermal conductivity (W/mK)
l = hydraulic radius of the solid body (m)
Nu = Nuselt number
P = pressure (Pa)
P_T = wetted perimeter of solid body (m)
Ra = Rayleigh number
S''' = volumetric entropy generation (W/m^3K)
T = temperature (K)
u = velocity in x-axis (m)
v = velocity in y-axis (m)
x = distance in x-axis (m)
y = distance in y-axis (m)

Greek symbols

α = thermal diffusivity (m^2/s)
β = expansion coefficient (K^{-1})
μ = viscosity ($N.s/m^3$)
υ = kinematic viscosity (m^2/s)
ρ = density (kg/m^3)

Subscripts

F = fluid
s = solid
w = wall
o = reference

Introduction

Mixed convection in a cavity receives considerable attention due to its importance in many engineering applications. Some of these include energy transfer in rooms and units, and cooling of industrial machines and electronic

International Journal of Numerical Methods for Heat & Fluid Flow, Vol. 10 No. 8, 2000, pp. 824-841.

Acknowledgements are due to King Fahd University of Petroleum and Minerals.

equipment. In mixed convection, heat transfer in flows in which the influence of forced convection and natural convection are of comparable magnitude. However, the ratio of Gr/Re^2 has been used to present the relative magnitudes of forced and natural convection in a mixed convection flows (Lloyd and Sparrow, 1970). Moreover, mixed convection flows may be further subdivided into those where the inertia force is parallel to the buoyancy force and those where the inertia force is perpendicular to the buoyancy force (Gebhart, 1971).

Considerable research studies were carried out on natural, mixed, and forced convection heat transfer. The combined force and natural convection heat transfer within a recirculating flow in an insulated lid-driven cavity of rectangular cross section was investigated by Prasad and Koseff (1996). The mean heat flux over the entire lower boundary was analyzed and the correlation for Nusselt and Stanton numbers was developed. They showed that the flow in the cavity was independent of Gr/Re^2 over the range studied. The numerical study on natural convection in a partitioned cubic enclosure was carried out by Karki and Sathyamurthy (1992). They explored the effects of various parameters on the flow structure and heat transfer. They indicated that the three-dimensional effects were significant for Rayleigh numbers considered in the study. Conjugate natural convection from an array of protruding heat source was investigated by Heindel *et al.* (1996). They showed that decreasing substrate thermal conductivity, fluid circulation decrease and the maximum heater temperature increased. Measurement of the turbulent velocity and temperature fields was carried out in a heated boundary layer downstream of a junction of a tapered cylinder and a wall. They indicated that the boundary layer was strongly affected by the presence of large-scale unsteadiness arising from vortex shedding. This appeared as turbulence with a strong spectral component at the shedding frequency. Natural convection in a square enclosure with a cold source was investigated by Chang and Tsai (1997). They modeled the air flow with two-dimensional consideration and k-e model was introduced to account for the turbulence. Their findings agreed with the literature. A numerical study was conducted for natural convection flow and heat transfer in a rectangular enclosure cooled from above with five discrete protruding heaters on a vertical wall by Ju and Chen (1996). They introduced a corrected Nusselt number when correlating their findings. They indicated that their findings agreed well with the experimental results. Mixed convection in a partially divided rectangular enclosure was studied numerically by Hsu *et al.* (1997). The simulation was extended for wide range of Reynolds and Grashof numbers. They indicated that the average Nusselt number and the dimensionless surface temperature depended on the location and height of the divider. Natural convection heat transfer from a discrete protruding copper block mounted on a vertical wall was studied experimentally by Darbhe and Muralidhar (1996). The buoyancy

flow around the protruding body was visualized using an interferrometric technique. They indicated that the local Nusselt number obtained was higher than its counterpart reported in the literature.

The entropy analysis enlightens the sources of irreversibility in the system and its minimization can be used to optimize the thermal system (Deniel and Kahraman, 1999). Transient exergy analysis and optimal removal time of a cylindrical storage system was investigated by Moweety and Rozani (1996). Their goal was to isolate different component of entropy production in the system as a function of the removal time. A numerical investigation of entropy generation for mixed convective flows in a vertical channel with transverse fin arrays was carried out by Cheng *et al.* (1977). They correlated the geometric configuration of the fin array with the entropy generation and suggested the arrangement of the fin arrays with minimum entropy generation. Entropic efficiency of energy system was investigated by Arpaci and Selamet (1992). They developed a fundamental relation between the Nusselt number describing heat transfer in any forced or buoyancy driven flow and the entropy production. Carrington and Sun (1992) studied second law analysis of combined mass and heat transfer in internal and external flows. They used a control volume method when establishing the role of entropy generation due to heat transfer and mass transfer in fluid stream. They demonstrated the application of the model developed in practical cases. Optimal paths for minimizing entropy generation in a common class of finite-time heating and cooling processes was investigated by Anderson and Gordon (1992). They compared the optimal paths with the common strategies of constant heat flux and constant source temperature operation. An entropy generation in fundamental convective heat transfer was studied by Bejan (1979). The second law aspects of heat transfer by forced convection were demonstrated in terms of four fundamental flow configurations. He showed how the flow geometric parameters might be selected in order to minimize the irreversibility associated with a specific convective heat transfer process. Yilbas *et al.* (1999) investigated the entropy generation due to swirling flow in pipes. They indicated that at high Prandtl numbers, the effect of swirling on the rate of entropy generation was significant.

The heat generating body aspect ratio in the cavity affects the heat transfer characteristics and irreversibility associated with the flow field. Some of the applications of such mixed convection systems are electronic device cooling, industrial product cooling, drying, etc. The thermal performance of such system depends on the exit and inlet port locations and the heat transferring body geometry. In this case, the heat transfer characteristics, as well as irreversibility generated in the system, can be improved by setting the proper inlet and exit port locations for a known heat releasing body geometry. In the present study, a heat generating solid body in a cavity with mixed convection is modeled, and heat transfer for a fixed inlet and variable exit conditions are investigated. In the simulations, air is

used as a fluid while steel is considered as heat generating body in the cavity. To investigate the influence of the heat generating body geometry on the heat transfer characteristics, two aspect ratios of the body are employed. In addition, five locations of the exit ports from each cavity wall are introduced provided that one inlet and one exit port are employed in each simulation. The irreversibility ratio is computed for each exit port location and each aspect ratio of the heat generating body.

Flow field and entropy formulation

The flow around the solid body with rectangular cross section in the cavity is assumed to be two-dimensional incompressible, laminar, and steady since the Reynolds number considered at present is in the order of 65. The governing equations of mass conservation, momentum and energy are given as follows.

Mass conservation equation:

$$\frac{\partial u}{\partial x}+\frac{\partial v}{\partial y}=0 \tag{1}$$

The momentum equation:
x-momentum

$$u\frac{\partial u}{\partial x}+v\frac{\partial u}{\partial y}=-\frac{1}{\rho}\frac{\partial p}{\partial x}+\upsilon\left(\frac{\partial^2 u}{\partial x^2}+\frac{\partial^2 u}{\partial y^2}\right) \tag{2}$$

y-momentum

$$u\frac{\partial v}{\partial x}+v\frac{\partial v}{\partial y}=-\frac{1}{\rho}\frac{\partial p}{\partial y}+\frac{g\beta\Delta T}{\rho}+\upsilon\left(\frac{\partial^2 v}{\partial x^2}+\frac{\partial^2 v}{\partial y^2}\right) \tag{3}$$

The energy equation

$$\rho C_p\left(u\frac{\partial T}{\partial x}+v\frac{\partial T}{\partial y}\right)=k\left(\frac{\partial^2 T}{\partial x^2}+\frac{\partial^2 T}{\partial y^2}\right)+\mu\phi \tag{4}$$

where

$$\phi=2\left[\left(\frac{\partial u}{\partial x}\right)^2+\left(\frac{\partial v}{\partial y}\right)^2\right]+\left[\frac{\partial v}{\partial x}+\frac{\partial u}{\partial y}\right]^2$$

Figure 1 shows the schematic view of the cavity, the solid body with aspect ratio 0.25, and the boundary conditions.

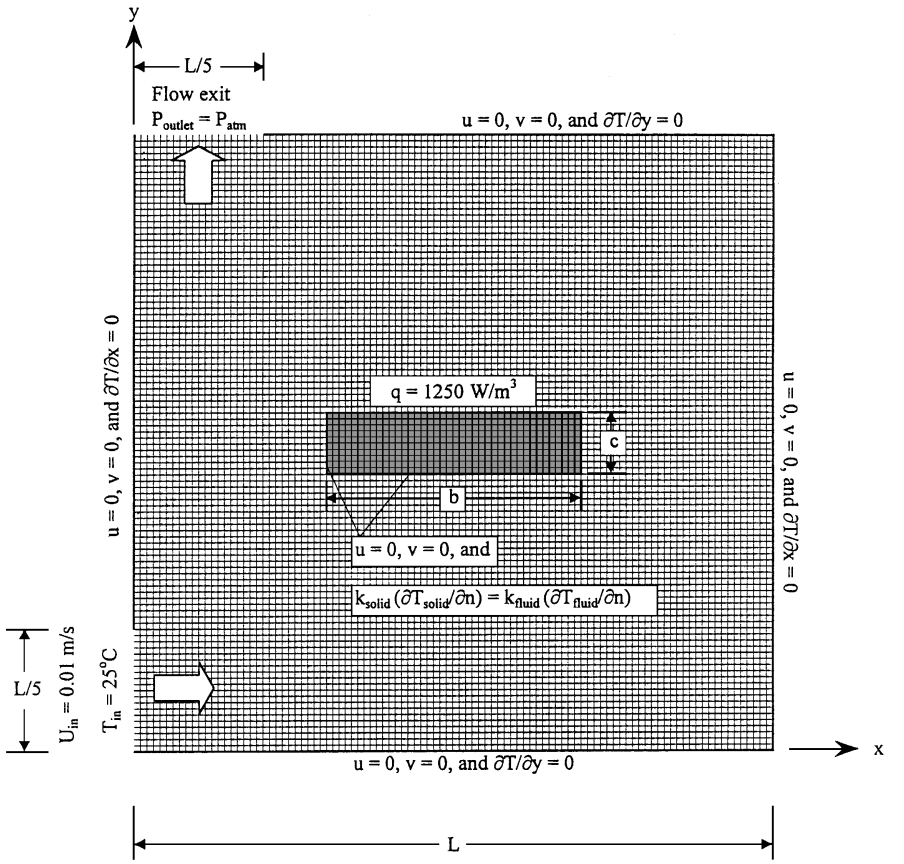

Figure 1.
Schematic view of the cavity and the solid body with the grid generated and boundary conditions for aspect ratio of 0.25, where L = 0.05m

Boundary conditions

At solid wall:

u = 0 and v = 0 (no slip condition)

At inlet and exit port of the cavity a uniform fluid temperature and uniform flow are assumed.

$$\frac{\partial \varphi}{\partial x} = 0 \quad \text{and} \quad \frac{\partial \varphi}{\partial y} = 0$$

where φ is any of the fluid property such as velocity and temperature.

Protruding solid body

Energy equation

$$k\left(\frac{\partial^2 T}{\partial x^2} + \frac{\partial^2 T}{\partial y^2}\right) + \dot{q}''' = 0 \tag{5}$$

where q''' is the uniform heat flux over the body.

Boundary conditions

At the solid wall

$$-k\frac{\partial T}{\partial n} = h(T_w - T_o)$$

and $T_s = T_f$

$$q''' = 1,250 \text{W/m}^3$$

Two aspect ratios of the solid body are considered provided that the areas under the solid body corresponding to both aspect ratios are same. The size of the protruding body can be formulated as:

$$b = 0.2\frac{L}{\sqrt{a}} \text{ and } c = 0.2\sqrt{aL}$$

where b and c are length and height of the protruding body, L is the length of cavity (L = 0.05 m) and a is the aspect ratio, which are 0.25 and 4.0. The inlet port of the cavity is fixed and the size of the exit port is the same size as the inlet port. The exit port location is altered along the cavity wall with equal distance. In this case, the exit port is situated in five locations in one wall of the cavity provided that in each simulation only one exit port is considered. Consequently, after the simulation the exit port location is moved a distance of L/5 away from its initial location, and the simulation is repeated for the new location of the exit port. Once the exit port is located at the last position in the side wall of the cavity, it is moved to first location of the neighbouring wall of the cavity, i.e. exit port location changes along the cavity walls by a distance L/5 after each simulation.

Dimensionless numbers:

Nusselt number:

$$Nu = \frac{hD}{k}$$

where,

$$h = \frac{\left(-k\frac{\partial T}{\partial n}\right)_{wall}}{(T_w - T_\infty)}$$

where n is the direction normal to the surface.

Grashof number:

$$\text{Gr} = \frac{\text{g}\beta\Delta\text{Tl}^3}{\upsilon^2}$$

Reynolds number:

$$\text{Re} = \frac{\text{V.l}}{\nu}$$

where l is the hydraluic radius of the solid body and $l = \frac{A}{P_T}$, where A is the cross-sectional area and P_T is the wetted perimeter of the solid body respectively.

Entropy analysis

The volumetric entropy generation is given in the previous study (Bejan, 1996) as:

$$\dot{S}'''_{\text{gen}} = \frac{k}{T^2}\left[\left(\frac{\partial T}{\partial x}\right)^2 + \left(\frac{\partial T}{\partial y}\right)^2\right] + \frac{\mu}{T}\left[\left\{\left(\frac{\partial u}{\partial x}\right)^2 + \left(\frac{\partial v}{\partial y}\right)^2\right\} + \left(\frac{\partial u}{\partial y} + \frac{\partial v}{\partial x}\right)^2\right] \tag{6}$$

where the first term is volumetric entropy generation due to heat transfer and the second term is due to fluid friction.

Irreversibility can be written as:

$$I = \int T_o \dot{S}'''_{gen} d\psi \tag{7}$$

In order to compare the effect of aspect ratio on the heat transfer and irreversibility generated, the following non-dimensional heat and irreversibility ratios are introduced:

$$\frac{I}{I_o} \text{ and } \frac{Q}{I}$$

where I_o is the maximum value of irreversibility generated in the cavity respectively.

Numerical solution

The flow domain is overlaid with a rectangular grid as shown in Figure 1. The control volume approach is employed in the numerical scheme. All the variables are computed at each grid point, except the velocities, which are determined midway between the grid points. The grid independent tests are conducted and 100 × 100 grid points are selected on the basis of less computation time without compromising the grid independency. A staggered grid arrangement is used in the present study, which provides the pressure linkages through the continuity equation and is known as SIMPLE algorithm (Patankar, 1980). This procedure is an iterative process for convergence. The pressure link between continuity and momentum is established by transforming the continuity equation into a Poisson equation for pressure. The Poisson equation implements a pressure correction for a divergent velocity field.

Results and discussions

The simulations are carried out for mixed flow conditions in a square cavity. The inlet port of the cavity is fixed while the exit port of the cavity is located at different positions in the cavity walls. The effect of exit port on the heat transfer characteristics and entropy generation are computed for two aspect ratios of the solid body and the resulting velocity, temperature and entropy contours are presented. The Rayleigh number used in the present simulation is 11,000. Table I gives the properties of the air and steel used in the simulations.

	Air	Steel
Density (Kg/m^3)	1.89	7,836
Specific heat (J/kg K)	1,005	969
Thermal conductivity (W/m K)	0.02565	28.2
Viscosity (m^2/s)	1.544×10^{-5}	–

Table I.
Properties of air and steel used in the simulations

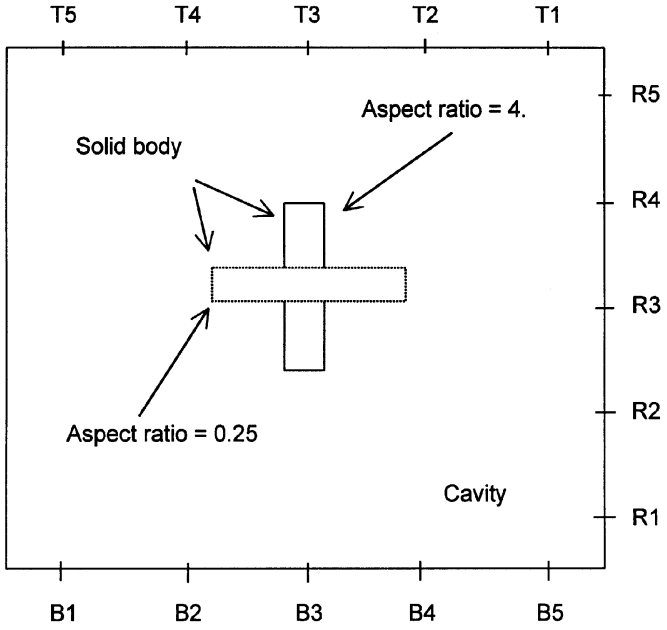

Exit port	Exit port Location #	Exit port	Exit port Location #	Exit port	Exit port Location #
T5	1	R5	6	B5	11
T4	2	R4	7	B4	12
T3	3	R3	8	B3	13
T2	4	R2	9	B2	14
T1	5	R1	10	B1	15

Figure 2.
Schematic view of exit port locations and corresponding numbers

The relative strength of the forced convection over natural convection can be judged on the base of Gr/Re^2, in the mixed convection. In this case, as Gr/Re^2 approaches unity, the buoyancy effect becomes important (Lloyd and Sparrow, 1970). Consequently, the natural convection dominates the mixed convection when $Gr/Re^2 >> 1$. Figure 3 shows the Gr/Re^2 variation with exit port locations for solid body with two aspect ratios while Figure 2 gives the schematic view of exit port locations and corresponding location numbers. When the exit port location number (Figure 2) is 5 and higher than 13, Gr/Re^2 increases indicating the dominant natural convection contribution in the mixed flow. This argument is true for both aspect ratios. Therefore, the influence of exit port location on the heat transfer characteristics is almost independent of the solid body aspect ratios provided that the aspect ratio of 4.0 (portrait configuration of the solid body) results in relatively higher Gr/Re^2 values as compared to its counter part resulted for aspect ratio of 0.25.

Figure 4 shows velocity contours in the cavity for different exit port locations and aspect ratio of 0.25. The orientation of circulation cells changes as

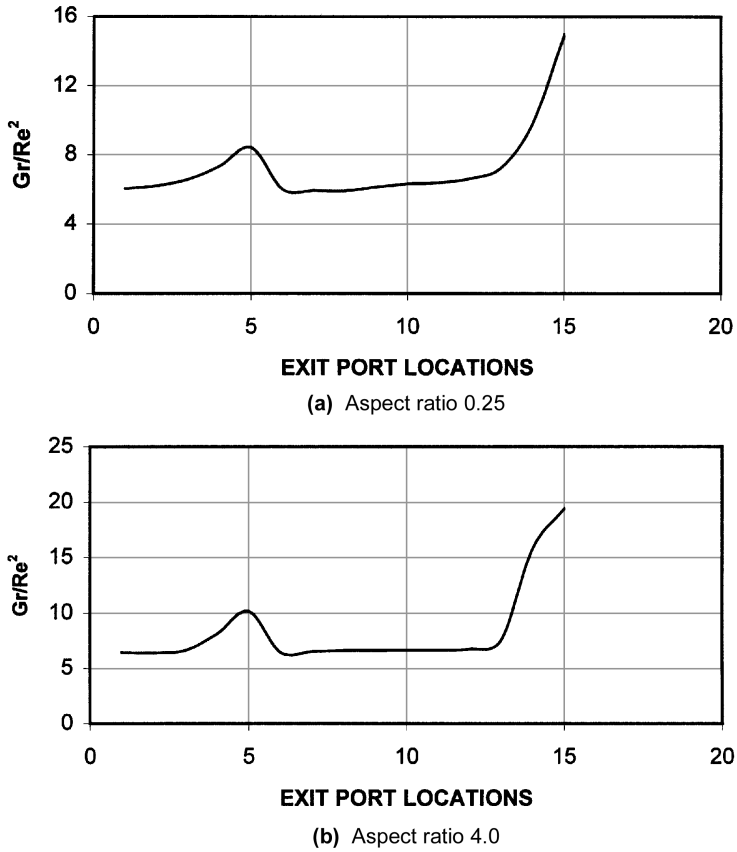

Figure 3.
Variation of Gr/Re^2 with exit port locations with aspect ratio of 0.25 and 4

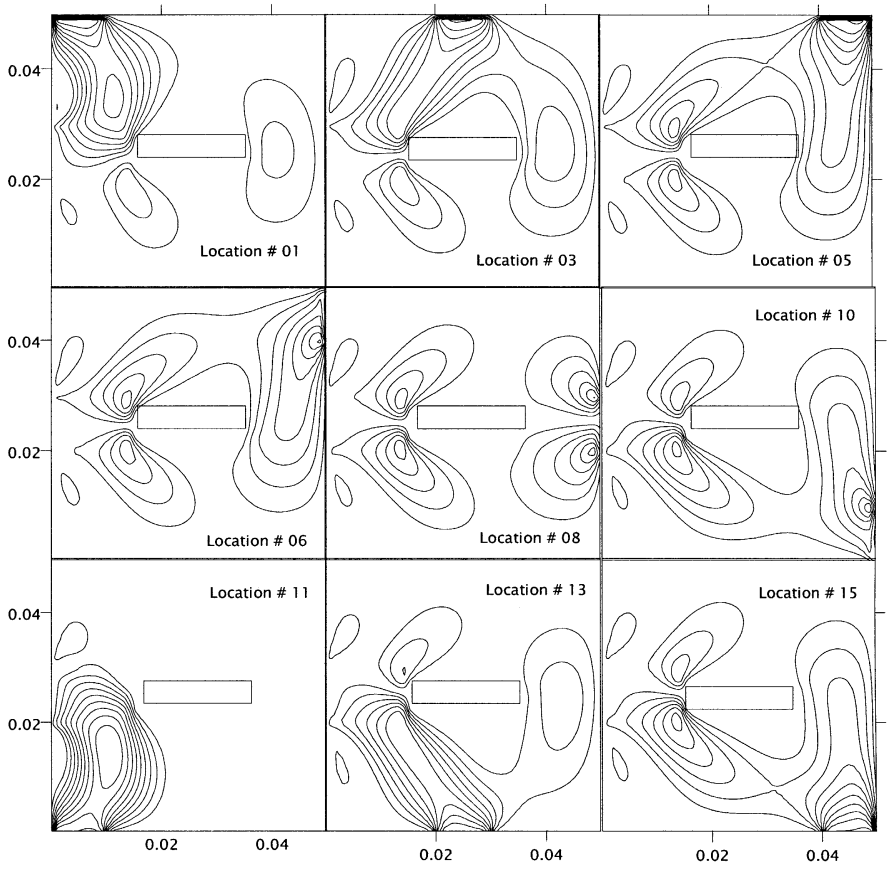

Figure 4.
Velocity contours at different exit port locations for aspect ratio of 0.25

the exit port location changes. The formation of circulation cells is because of the mixing of the fluid due to buoyancy driven and convective currents. The size of the circulation cells increases when exit port is situated at either 5, 10 or 15 exit port location numbers as shown in Figure 2. It should be noted that Gr/Re^2 increases at exit port location numbers of 5, 10 and 15, which indicates the domination of the buoyancy current (due to natural convection) in the flow field. Therefore, as the buoyancy current increases, the size of the circulation cell increases. Moreover, two circulation zones below and above the solid body front surface are formed for all exit port locations. The circulation zone above the solid body front surface is because of the buoyancy current developed in this region. The size of this circulation cell increases when the exit port is located in the upper wall of the cavity. This occurs because the convective and buoyancy currents are in the same direction. Consequently, the convective current contribution on the size of the circulation cell signifies when the buoyancy and convective currents are in the same direction.

Figure 5 shows the temperature contours in the cavity for different exit port locations and the solid body aspect ratio of 0.25. The temperature contours follow almost the velocity contours provided that no circulation zones are identified by the temperature contours. The effect of convective current on the temperature contours is visible, since the temperature contours extend towards the exit port. In addition, this extension of temperature contours is also apparent for the exit port location in the lower wall of the cavity.

When comparing the temperature contours corresponding to same exit port locations where one is in the upper and the other in the lower walls of the cavity, it can be observed that both temperature contours are not symmetrical. This is because of the buoyancy current generated; in which case, the temperature contours are more coherent when the buoyancy and convective current are in the same direction. Moreover, the temperature contours extends from the top surface of the solid body further inside the cavity when exit port location is in the lower wall of the cavity. This suggest that the buoyancy

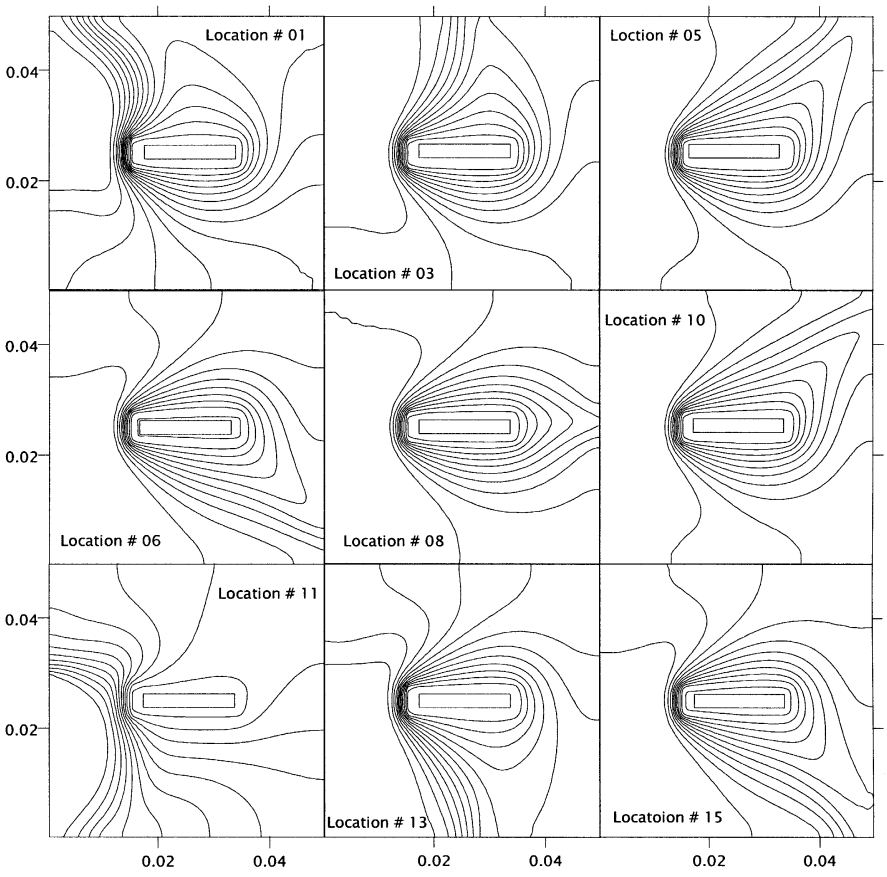

Figure 5.
Temperature contours at different exit port locations for aspect ratio of 0.25

driven current enables to heat the fluid above the solid body although the convective current is dominated below the solid body in the cavity. This also indicates the enhanced contribution of the natural convection cooling of the solid body, which may also be seen from Figure 3 in which Gr/Re^2 is shown with exit port locations, i.e. natural convection from the surface of the solid body, except the bottom surface dominates over the forced convection for the exit port locations in the lower wall of the cavity.

Figure 6 shows the entropy contours in the cavity for different exit port locations and solid body aspect ratio of 0.25. The entropy generation includes the heat transfer and viscous effects. The entropy generation is high in the front surface of the solid body and it extends towards the lower side of the solid body. This is mainly because of the heat transfer contribution to the entropy generation than the viscous dissipation, since the ratio of heat transfer to viscous dissipation contribution of entropy is considerably high.

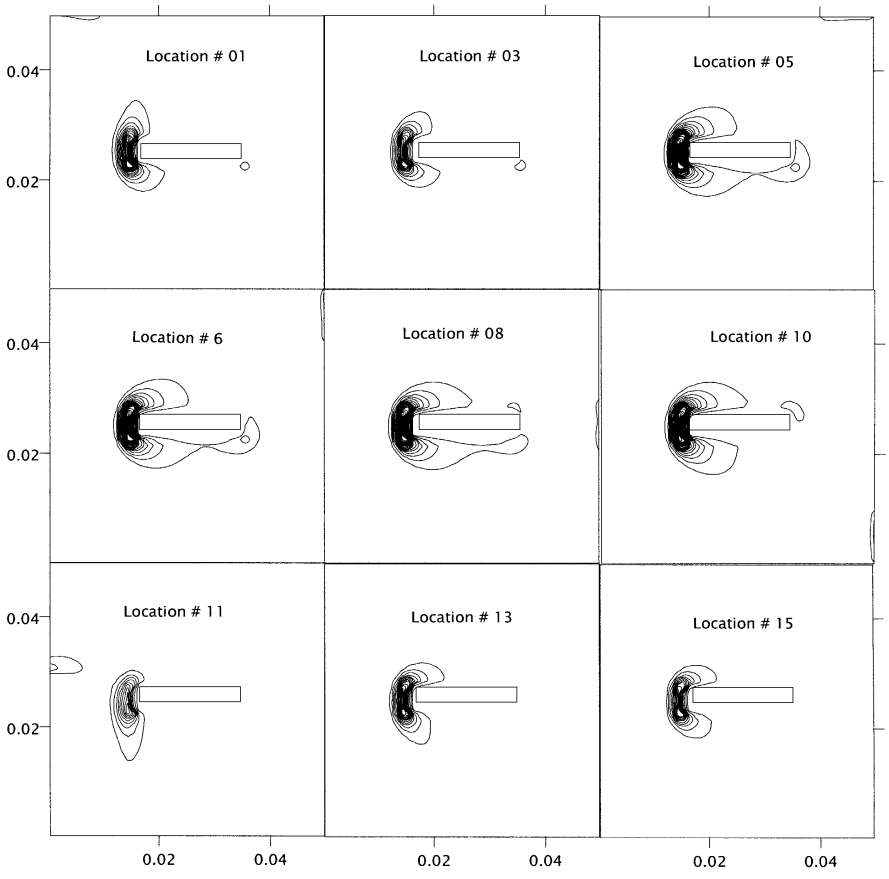

Figure 6.
Entropy contours at different exit port locations for aspect ratio of 0.25

In this case, the temperature gradient changes sharply in the region close to the front surface of the solid body due to the thin thermal boundary layer developed in this region, which is evident from temperature contours. It should be noted that the entropy generation in the whole cavity is not zero, but the contours corresponding to relatively large entropy generation are shown in the Figure 6.

Figure 7 shows the normalized overall Nusselt number $(Nu/Nu_o)_{overall}$ with the exit port locations for two different aspect ratios of the solid body while Figure 8 shows the $Nu/Gr/Re^2$ variation with exit port locations. $(Nu/Nu_o)_{overall}$ decreases generally with increasing exit port location numbers. $(Nu/Nu_o)_{overall}$ reduces to reach local minimum for exit port number 5. In this case, the rate of heat transfer from the solid body reduces. Moreover, it is also evident from Figure 3 that the Gr/Re^2 attains local maximum at exit port location 5.

Therefore, the natural convection contribution in heat transfer characteristics substantiates at this exit port location. Consequently, as the natural convection contribution increases, the rate of heat transfer from the

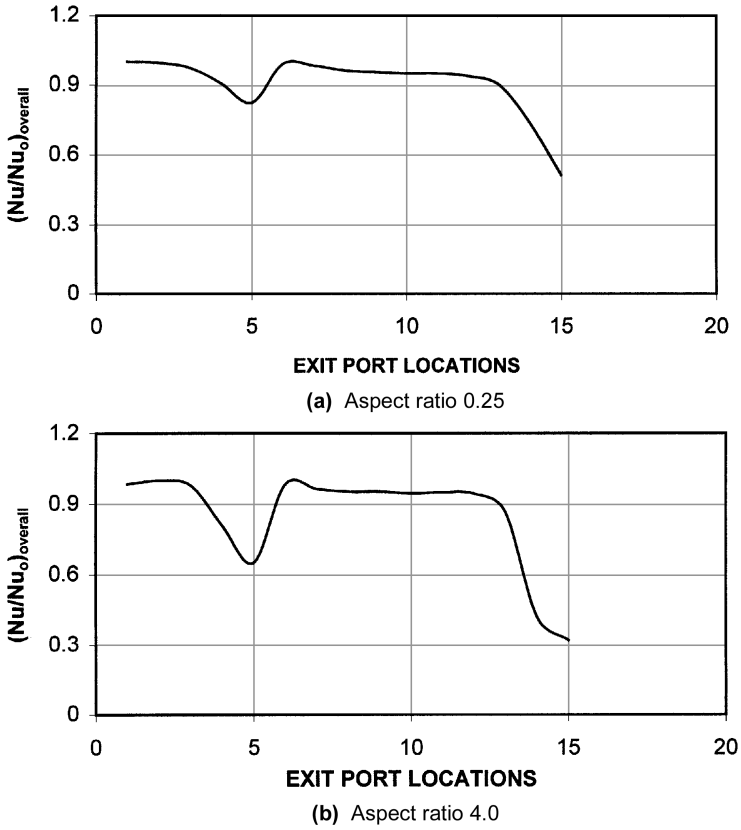

Figure 7.
Variation of $(Nu/Nu_o)_{overall}$ with exit port locations for aspect ratios of 0.25 and 4

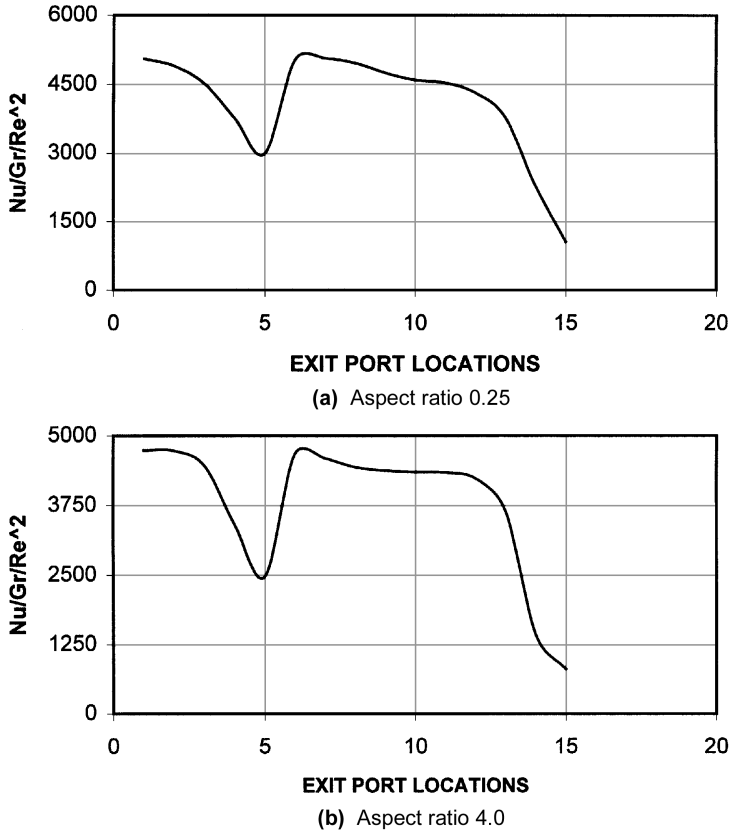

Figure 8. Variation of $Nu/Gr/Re^2$ with exit port locations for aspect ratios of 0.25 and 4

solid body reduces, i.e. as Gr/Re^2 increases $(Nu/Nu_o)_{overall}$ decreases. The effect of the aspect ratio of the solid body on the $(Nu/Nu_o)_{overall}$ profile along the exit port location is not significant provided that $(Nu/Nu_o)_{overall}$ reduces slightly in the case of aspect ratio of 0.25 as Gr/Re^2 increases. This is because of the different velocity and temperature field attainment in the cavity for different aspect ratios. Therefore, for both aspect ratios, the rate of heat transfer from the solid body reduces as the exit port location number increases beyond 12, i.e. exit port locations in the lower wall of the cavity reduce the rate of heat transfer from the solid body.

Figure 9 shows the normalized irreversibility ratio (I/I_o) with exit port location numbers for two different aspect ratios. In general, I/I_o increases with increasing exit port location numbers for both aspect ratios. This is more pronounced for the exit port location number 13 and more. This is because the viscous losses as well as the temperature gradient in the cavity increase, i.e. the heat dissipation in the cavity is non-uniform, which in turn results in non-uniform temperature distribution in the cavity. The increase in irreversibility does not depend significantly on the aspect ratio of the solid body.

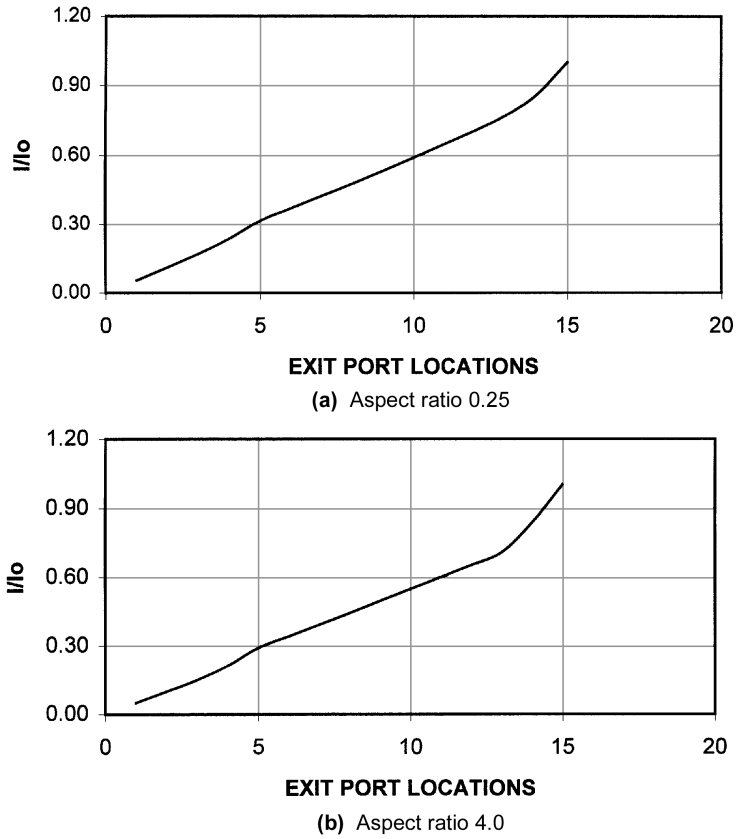

Figure 9.
Variation of I/I_0 with exit port locations for aspect ratios of 0.25 and 4

Figure 10 shows the irreversibility to heat transfer ratio. I/Q attains low values for the exit port location number of 1 to 13. As the exit port location number increases further I/Q also increases. This is because the irreversibility increases while heat transfer reduces for large exit port location number. Moreover, I/Q attains relatively higher values for the aspect ratio of 4 as compared to its counter part corresponding to the aspect ratio of 0.25. This is again due to the irreversibility generated and heat transfer taking place in the cavity for each aspect ratio. Nevertheless, the difference between I/Q due to two aspect ratios is not substantial.

Conclusions

The mixed flow conditions are simulated for two aspect ratios of rectangular solid body in a square cavity. The effect of exit port locations on the irreversibility and heat transfer characteristics are examined. In general, the natural convection contribution of the heat transfer enhances as the exit port location numbers increase beyond 13. The irreversibility increases as the

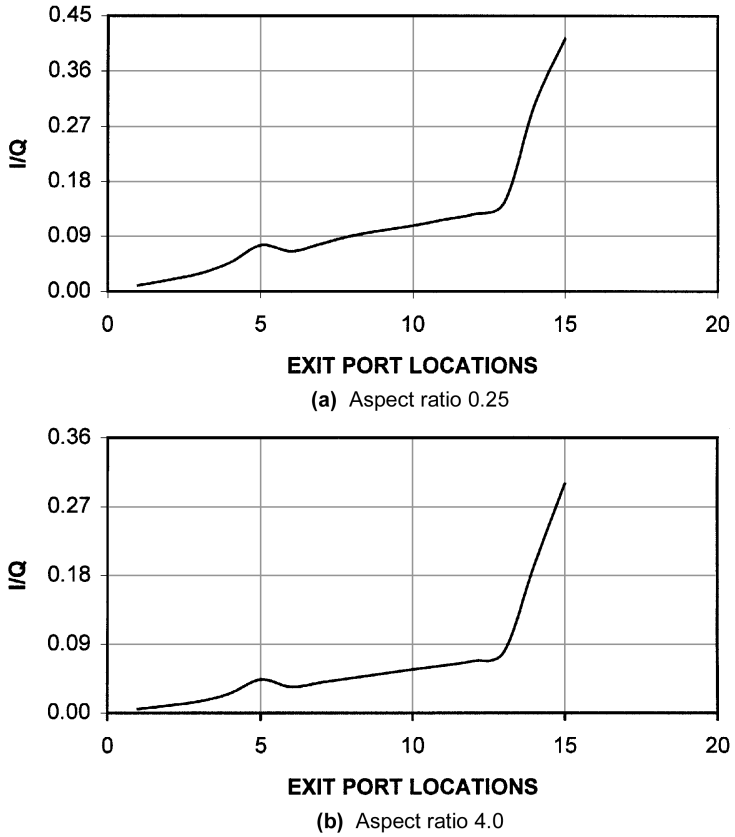

Figure 10. Variation of I/Q with exit port locations for aspect ratios of 0.25 and 4

exit port location number increases. Moreover, the irreversibility to heat transfer ratio improves (reduces) for low exit port location numbers. The specific conclusions derived from the present work can be listed as follows:

- The flow field in the cavity changes its mode as the exit port location changes. In this case, the buoyancy driven current generates large circulation cells for large exit port location numbers. However, the mixing of the buoyancy driven and convective current generates a circulation between the front surface of the solid body and the front cavity wall. This becomes more visible when the exit port locations are in the top and side walls of the cavity. The effect of aspect ratio on the velocity field is more pronounced for the large exit port location numbers.
- The temperature contours follow almost the velocity contours provided that no circulation zone is identified from the temperature contours. The temperature contours, in general, extend towards the exit port due to convective and buoyancy driven currents. The temperature contours

from the top and side surfaces of the body extend further inside the cavity when the exit port locations are in the bottom wall of the cavity. This is because of the natural convection heat transfer contribution in these regions.

- The overall normalized Nusselt number $(Nu/Nu_o)_{overall}$ reduces as the exit port location number increases beyond 13. This argument is true for both aspect ratios. This may indicate that as the natural convection heat transfer contribution enhances, $(Nu/Nu_o)_{overall}$ reduces. This is more pronounced when the exit ports are located in the bottom wall of the cavity.
- The normalized irreversibility increases as the exit port location number increases beyond 13. Moreover, the irreversibility to heat transfer ratio attains low values for low exit port location numbers. In this case, the heat transfer from the solid body enhances while the irreversibility reduces.

References

Anderson and Gordon, J.M. (1992), "Optimal paths for minimizing entropy generation in a common class of finite time heating and cooling processes", *Int. J. Heat and Fluid Flow*, Vol. 13, pp. 294-9.

Arpaci, V.S. and Selamet, A. (1992), "Entropic efficiency of energy systems," *Prog. Energy Combust. Sci.*, Vol. 18, pp. 429-45.

Bejan, A. (1979), "A study of entropy generation in fundamental convective heat transfer," *ASME, J. Heat Transfer*, Vol. 101, pp. 718-25.

Bejan, A. (1996), *Entropy Generation Minimization*, CRC Press, Florida.

Carrington, G. and Sun, Z.F. (1992), "Second law analysis of combined heat and mass transfer in internal and external flows", *Int. J. Heat and Fluid Flow*, Vol. 13, pp. 65-70.

Chang, Y.P. and Tsai, R. (1997), "Natural convection in a square enclosure with a cold source", *Int. Comm. Heat Mass Transfer*, Vol. 24, pp. 1019-27.

Chen, J.S., Sparrow, E.M. and Mocooglu, A. (1977), "Mixed convection in a boundary layer flow on a horizontal plate", *ASME J. Heat Transfer*, Vol. 99, pp. 66-71.

Darbhe, M.N. and Muralidhar, R. (1996), "Natural convection heat transfer from a discrete protruding surface", *Int. Comm. Heat Mass Transfer*, Vol. 23, pp. 417-26.

Deniel, Y. and Kahraman, R. (1999), "Entropy generation in a rectangular packed duct with wall heat flux", *Int. J. Heat and Mass Transfer*, Vol. 42, pp. 2337-44.

Gebhart, B. (1971), *Heat Transfer*, 2nd ed., McGraw-Hill, New York, NY, pp. 388-97.

Heindel, T.J., Ramadhyani, S. and Incropera, F.P. (1996), "Conjugate natural convection from an array of protruding heat sources", *Numerical Heat Transfer, Part A*, pp. 1-18.

Hsu, T., Hsu, P. and How, S. (1997), "Mixed convection in a partially divided rectangular enclosure", *Numerical Heat Transfer, Part A*, Vol. 31, pp. 655-83.

Ju, Y. and Chen, Z. (1996), "Numerical simulation of natural convection in an enclosure with discrete protruding body heaters", *Numerical Heat Transfer, Part A*, Vol. 30, pp. 207-18.

Karki, K.C. and Sathyamurthy, P.S. (1992), "Natural convection in a partitioned cubic enclosure," *ASME, J. Heat Transfer*, Vol. 114, pp. 410-17.

Lloyd, J.R. and Sparrow, E.M. (1970), "Combined forced and free convection flow on vertical surfaces", *Int. J. Heat Mass Transfer*, Vol. 13, pp. 434-8.

Moweety J.G. and Razani, A. (1996), "A two-dimensional numerical investigation of the optimal removal time and entropy generation rate for a sensible thermal storage system", *Energy, The International Journal*, Vol. 21, pp. 1265-76.

Patankar, S.V. (1980), *Numerical Heat Transfer and Fluid Flow*, Hemisphere Publishing Comp., Washington, DC.

Prasad, K. and Koseff, J.R. (1996), "Combined forced and natural convection heat transfer in a deep lid-driven cavity flow", *Int. J. Heat and Fluid Flow*, Vol. 17, pp. 460-7.

Yilbas, B.S., Shuja, S.Z. and Budair, M.O. (1999), "Second law analysis of a swirling flow in a circular duct with restriction", *Int. J. Heat and Mass Transfer*, Vol. 42, pp. 4027-41.